Bioactive Materials 6 (2021) 2439–2451

Contents lists available at ScienceDirect

Bioactive Materials

journal homepage: www.sciencedirect.com/journal/bioactive-materials

Excavating bioactivities of nanozyme to remodel microenvironment for protecting chondrocytes and delaying osteoarthritis

Weiduo Hou [a,d,1], Chenyi Ye [a,d,1], Mo Chen [e,1], Wei Gao [c], Xue Xie [c], Jianrong Wu [b], Kai Zhang [f], Wei Zhang [a,d,**], Yuanyi Zheng [c,*], Xiaojun Cai [b,***]

[a] Department of Orthopaedics, Second Affiliated Hospital, School of Medicine, Zhejiang University, 310009, Hangzhou, China
[b] Shanghai Institute of Ultrasound in Medicine, Shanghai Jiao Tong University Affiliated Sixth People's Hospital, Shanghai, 200233, PR China
[c] Department of Ultrasound in Medicine, Shanghai Jiao Tong University Affiliated Sixth People's Hospital, Shanghai, 200233, PR China
[d] Research Institute of Orthopaedics, Zhejiang University, 310009, Hangzhou, China
[e] Department of Rheumatology, Second Affiliated Hospital, School of Medicine, Zhejiang University, 310009, Hangzhou, China
[f] Laboratory for Pathophysiological and Health Science, RIKEN Center for Biosystems Dynamics Research, Kobe, Hyogo, 650-0047, Japan

ARTICLE INFO

Keywords:
Reactive oxygen species
Prussian blue nanozyme
Arthritis
Inflammation
Chondrocytes

ABSTRACT

Osteoarthritis (OA) is the main cause of disability in the elderly. Effective intervention in the early and middle stage of osteoarthritis can greatly prevent or slow down the development of the disease, and reduce the probability of joint replacement. However, there is to date no effective intervention for early and middle-stage OA. OA microenvironment mainly destroys the balance of oxidative stress, extracellular matrix synthesis and degradation of chondrocytes under the joint action of biological and mechanical factors. Herein, hollow Prussian blue nanozymes (HPBzymes) were designed via a modified hydrothermal template-free method. The aim of this study was to investigate the effects of HPBzymes on chondrocytes and the progression of OA. The intrinsic bioactivities of HPBzymes were excavated *in vitro* and *in vivo*, remodeling microenvironment for significantly protecting chondrocytes and delaying the progression of traumatic OA by inhibiting reactive oxygen species (ROS) and Rac1/nuclear factor kappa-B (NF-κB) signaling in a rat model. HPBzyme significantly diminished interleukin (IL)-1β-stimulated inflammation, extracellular matrix degradation, and apoptosis of human chondrocytes. HPBzyme attenuated the expression of Rac1 and the ROS levels and prevented the release and nuclear translocation of NF-κB. Deeply digging the intrinsic bioactivities of nanozyme with single component to remodel microenvironment is an effective strategy for ROS-associated chronic diseases. This study reveals that excavating the bioactivities of nanomedicine deserves attention for diagnosis and treatment of severe diseases.

1. Introduction

Osteoarthritis (OA) is the main cause of disability in the elderly [1]. OA is becoming more common as the population ages and the prevalence of obesity increases [2]. In clinic, the treatment of early OA is typically based on non-pharmacological and pharmacological treatments. Non-pharmacological strategy mainly include physical activity [3] and nutrition [4]. Non-steroidal anti-inflammatory agents or intra-articular injection of hyaluronic acid and corticosteroids [5]. Although these drugs alleviate pain and symptoms, they cannot delay disease progression [6], and have side effects, such as damage to the digestive and cardiovascular systems [7]. Artificial joint arthroplasty is effective for patients with end-stage OA [8]. However, because of the wear, cost, and invasiveness of artificial joints, they are mainly suitable for patients with severe symptoms of late OA [9]. Effective intervention in the early and middle stage of osteoarthritis can greatly prevent or slow down the development of the disease, and reduce the probability of joint replacement [10]. However, there is to date no effective

Peer review under responsibility of KeAi Communications Co., Ltd.
* Corresponding author.
** Corresponding author. Department of Orthopaedics, Second Affiliated Hospital, School of Medicine, Zhejiang University, 310009, Hangzhou, China.
*** Corresponding author.
E-mail addresses: zhangweilook@zju.edu.cn (W. Zhang), zhengyuanyi@sjtu.edu.cn (Y. Zheng), 981637680@qq.com (X. Cai).
[1] Weiduo Hou, Chenyi Ye, and Mo Chen contributed equally to this work.

https://doi.org/10.1016/j.bioactmat.2021.01.016
Received 15 November 2020; Received in revised form 18 December 2020; Accepted 12 January 2021

intervention for early and middle-stage OA [11].

Microenvironment is an important factor to maintain joint homeostasis. OA is primarily characterized by the damage of cartilage, largely resulting from hostile microenvironment [12]. OA mircoenvironment mainly destroys the balance of oxidative stress, extracellular matrix (ECM) synthesis and degradation of chondrocytes and subchodral bone under the joint action of biological and mechanical factors. These processes lead to degeneration and fibrosis of articular cartilage, subchondral osteosclerosis, peripheral hyperosteogeny, joint space narrowing and synovitis [13,14]. Growing evidence reveals that OA microenvironment includes excessive inflammation [15,16], matrix metalloproteases (MMPs) overexpression [17], oxidative stress and the overproduction of reactive oxygen species (ROS) [12,18,19]. The most important aspect of OA is the degeneration of articular cartilage [20]. Articular cartilage is predominantly composed of ECM with chondrocytes. Chondrocytes secrete collagen, aggrecan, elastin, and other ECM components. The majority of cartilage ECM is composed of COL2 and proteoglycan, and it protects the integrity of bone and maintains cartilage tension and compressive properties [21]. Chondrocyte apoptosis and ECM degradation are the most important characteristic pathological changes in OA [22,23]. ROS are free radicals and are involved in diverse biological processes [19]. Oxidative stress and ROS are closely related to the pathogenesis of OA, and result in MMPs production, ECM degradation, joint inflammation and chondrocyte apoptosis [12,19,24]. ROS modulate cartilage metabolism, chondrocyte apoptosis, ECM synthesis and decomposition, and cytokine production [18]. The balance of ROS and antioxidants is linked to the occurrence, development, and progression of OA. Overproduced ROS is involved in various signaling pathways activated by injury or cytokines, amplifying inflammation and accelerating chondrocyte catabolism and apoptosis [25]. H_2O_2 and inflammation induce excess ROS production by chondrocytes [26]. Manganese ferrite and ceria nanoparticle-anchored mesoporous silica nanoparticles with methotrexate ameliorated rheumatoid arthritis, by scavenging ROS and inducing M2 macrophages Polarization [27]. However, its multiple components, complex preparation, and potential *in vivo* toxicity diminish the clinical potential. In the OA microenvironment, the levels of inflammatory mediators such as chemokines, adipokines and proinflammatory factors (IL-6 COX-2, and inducible nitric oxide synthase [iNOS]) are elevated [28]. Remodeling joint microenvironment may be a potential therapeutic strategy for OA [19].

Compared with conventional enzymes, nanozymes are a special kind of nano-materials with intrinsic enzyme-like activities, exhibiting their own unique advantages, such as multifunctionality and efficiency [29–32]. Xi et al. revealed that a nanozyme-based artificial peroxisome ameliorated hyperuricemia and ischemic stroke [33]. Liu et al. showed that an integrated cascade nanozyme with a formulation of Pt@PCN222–Mn was developed to eliminate excessive ROS to treat inflammatory bowel disease [34]. Prussian blue is an antidote approved by the United States Food and Drug Administration (FDA) for poisoning by radioactive Cs^+ or non-radioactive Tl^+ and shows good biocompatibility and biosafety [35,36]. Based on their intrinsic anti-inflammatory and anti-oxidative bioactivities, PBzymes have been investigated as therapeutics for lipopolysaccharide induced inflammation, inflammatory bowel disease, and ischemic stroke [37–40]. The peroxidase, catalase, and superoxide dismutase (SOD) activities of PBzymes mediate their scavenging of •OH, •OOH, and H_2O_2 [39,41]. ROS scavenging property of PBzymes is mediated by electron transport. In addition, PBzymes can be applied for cancer theranostics, as biosensors, and for treating inflammatory diseases [36,40,42]. May PBzymes take full advantage of their intrinsic properties to remodel OA microenvironment, providing guarantee for normal growth and recovery of bone and joint? It is also of great significance to reveal the bioactivities of PBzyme in the treatment of OA, providing an alternative efficient strategy to develop new OA drug.

Herein, a nanozyme-mediated microenvironment remodeling strategy to protect chondrocytes and delay OA was proposed. The aim of this research was to reveal the effects of PBzymes on chondrocytes and the progression of OA. A modified hydrothermal templet-free method was selected to achieve hollow PBzymes (HPBzymes) with mesoporous structure and high specific surface area (Fig. 1a). HPBzymes with single component and the intrinsic bioactivities were selected to illustrate the proposed strategy of remodeling microenvironment for treatment of OA. Human chondrocytes and the traumatic-induced OA rat were adopted as *in vitro* and *in vivo* models, respectively. The bioactivities of HPBzyme were excavated in the treatment of OA detailedly both *in vitro* and *in vivo*. HPBzyme protected chondrocytes, mitigated the inflammatory response, prevented chondrocyte ECM degradation, and exhibited therapeutic efficacy *in vivo* (Fig. 1b). The underlying biological mechanism was the inhibition of the Rac1/ROS/nuclear factor-kappaB (NF-κB) signaling pathway to remodel microenvironment of OA (Fig. 1b). This work provides a promising avenue for treatment of OA and even ROS-associated chronic diseases, that is deeply digging the intrinsic bioactivities of nanozyme with single component to remodel microenvironment.

2. Experimental section

2.1. Characterization of HPBzyme

The microstructure and physical characteristics of HPBzyme were visualized using a JEM-2100F TEM and scanning transmission electron microscope (STEM). The crystal properties were assessed by X-ray diffraction (Rigaku D/MAX-2200PX). The chemical bonds was characterized by Fourier transform infrared spectroscopy. The size of HPBzyme was measured by Dynamic light scattering (Nano ZS90 Zetasizer, Malvern). The absorption spectrum was recorded using Shimadzu UV-3600 ultraviolet–visible spectrophotometer.

2.2. Preparation of HPBzyme

PVP (125 g), $K_3[Fe(CN)_6]$ (12.375 g), and $Bi(NO)_3$ (2.45 g) were mixed and dissolved in nitric acid (1 M, 1000 mL). The solution was clarified by magnetic stirring for 40 min, then placed in an oven at 80 °C for 20 h, and HPBzyme was isolated by centrifugation, separation, and washing for three times with acetone and deionized water. The isolated HPBzyme was achieved via a vacuum freezing drying process.

2.3. Scavenging of •OH by HPBzyme

To study the scavenging of •OH by PBzyme, electron spin resonance (ESR) was performed to evaluate the spectra of •OH with a TiO_2/UV system. TiO_2 generates •OH under 340 nm UV light. HPBzyme with various concentrations was added to TiO_2 (0.1 mg/mL) and 50 mM BMPO. The ESR spectra were recorded under the following conditions: 20 mW microwave power, 1 G field modulation, and 200 g scan width. Samples were irradiated with UV light at 340 nm for 5 min.

2.4. Scavenging of •OOH by HPBzyme

To examine •OOH scavenging by HPBzyme, 1 mM xanthine and 0.2 U/mL xanthine oxidase were mixed for 1.5 min, and BMPO was spin-adducted with •OOH to form BMPO/•OOH adduct. HPBzyme with various concentration was added to the xanthine/xanthine oxidase (XO/XOD) system and assayed using a Bruker EMX spectrometer.

2.5. Scavenging of H_2O_2 by HPBzyme

HPBzyme reduces H_2O_2 to water: $2H_2O_2 \rightarrow O_2 + 2H_2O$. The activity of HPBzyme was assessed using a DZS-708 multi-parameter analyzer at room temperature. After automatic calibration with oxygen-free solution, 0.1 mL HPBzyme buffer (pH 7.4) was added to 1 mL 30% H_2O_2, and

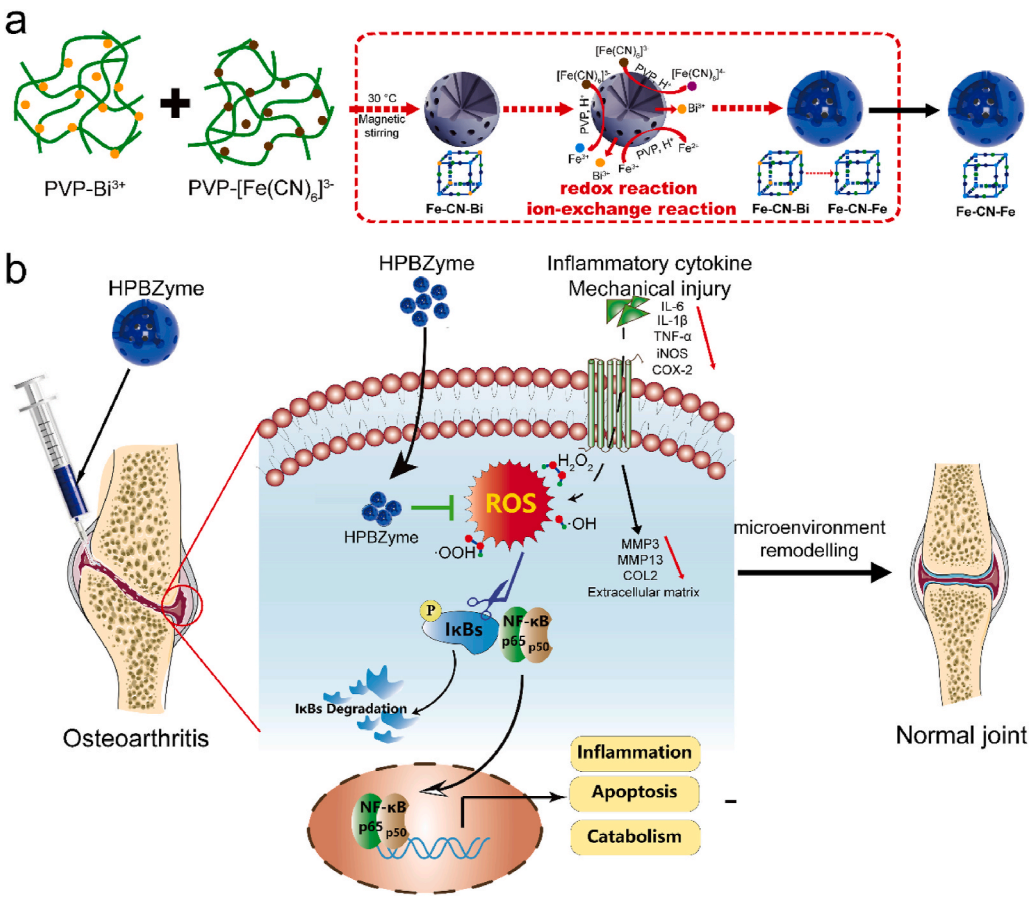

Fig. 1. **(a)** The diagrammatic sketch of the synthesis of HPBzyme. **(b)** Schematic diagram of the mechanism by which HPBzyme protects chondrocytes and delays arthritis. HPBzyme remodels the microenvironment of OA through attenuating proinflammatory cytokine/mechanical injury-induced inflammation, reducing extracellular matrix catabolism, and preventing chondrocyte apoptosis via inhibiting the ROS and Rac1-NF-κB signaling. HPBzyme provides a good environment for the recovery of OA via remodeling the OA microenvironment, showing therapeutic potential for OA.

oxygen generation was measured using an oxygen electrode. In addition, ESR spin-label oximetry was performed to evaluate the CAT-like mimetics of HPBzyme. 3-Carbamoyl-2,2,5,5-tetra-methyl-3-pyrroline-1-yloxyl (CTPO) is highly sensitive to changes in oxygen concentration (*58*, *59*). The ESR spectrum of CTPO depends on the number of O_2 molecules interacting with spin markers [43]. The spectrum of CTPO shows a hyperfine structure because of the interaction between the unpaired electrons of oxygen and the nitrogen nucleus of CTPO. As the O_2 concentration increases, physical collision between CTPO and O_2 reduces the peak intensity and broadens the spectral line width. The ESR detection parameters were microwave power, 1.0 mW; modulation amplitude, 0.04 G; and scan range 5 G [41]. The solutions used were 25 mM H_2O_2 and 0.1 mM CTPO in PBS (pH 7.4). The sample solutions were deoxygenated with nitrogen for 10 min, and H_2O_2 was added. PBzyme solution was added, and after 2 min the oxygen produced was assayed. To explore the relationship between O_2 generation and reaction time, 25 mM H_2O_2, 0.1 mM CTPO, and HPBzyme were mixed for various time. The O_2 concentration was determined by measuring the K parameter and calculated by the following equation: $10^4[O_2] = 2.30–7.46K$.

2.6. Isolation and stimulation of chondrocytes

This study was performed in accordance with the principles of the Basel Declaration and the recommendations of Zhejiang University; the Ethics Committee of Zhejiang University approved the protocol (No. 2017042). Normal human chondrocytes were isolated from patients with femoral neck fractures who underwent hip arthroplasty in our Orthopedic Trauma Department (four patients, median age 66 years, range 63–71 years). None of the subjects had a history of inflammatory disease or arthritis. Following a prior study [44], cartilage was cut into 1 mm^3 pieces and immediately digested with 0.2% collagenase II with shaking at 37 °C for ~12 h with 2% oxygen. The chondrocytes were seeded in a 10 cm^2 dish and cultured in low-glucose Dulbecco's modified Eagle's medium: F12 1:1 with 10% fetal bovine serum. Cells at passages 1–3 were used. To confirm the chondrogenic phenotype, chondrocyte markers were assayed according to a previous study [45] (Fig. S5).

Before stimulation, cells were pretreated with medium without fetal bovine serum for 1 day. Where indicated, the cells were incubated with 10 ng/mL recombinant IL-1β (R&D Systems).

2.7. Cell Counting Kit-8 assay

To evaluate the impact of HPBzyme on cytotoxicity, chondrocytes were treated with HPBzyme and incubated with 10% Cell Counting Kit-8 (CCK-8) solution (Dojindo, Kumanoto, Japan) for 3 h at 37 °C. The absorbance at 450 nm was measured using a microplate reader.

2.8. Flow cytometry for detection of apoptosis

Chondrocytes were incubated with 4 mM H_2O_2 and/or HPBzyme for 1 day [46], dispersed, and collected. The cells were incubated with 10 μL PE-enhanced green fluorescent protein (KeyGEN BioTECH, China) and 5 μL propidium iodide (KeyGEN BioTECH) for 20 min protected from light. Finally, the samples were analyzed by flow cytometry.

2.9. Quantitative real-time polymerase chain reaction

cDNA was prepared as described previously [47]. Using the Power SYBR® Green PCR Master Mix (TaKaRa Bio, Kutsatsu, Japan), mRNA levels were assayed using the ABI StepOnePlus™ System. The housekeeping gene was GAPDH. The primers were designed and prepared by Sangon Biotech Inc. (Shanghai, China). The primers used were as

follows: GAPDH, Forward: GGAGCGAGATCCCTCCAAAAT; Reverse: GGCTGTTGTCATACTTCTCATGG; IL6, Forward: ACTCACCTCTTCAGAACGAATTG; Reverse: CCATCTTTGGAAGGTTCAGGTTG; iNOS, Forward: AGGGACAAGCCTACCCCTC; Reverse: CTCATCTCCCGTCAGTTGGT. The $2^{-\triangle\triangle}$ Ct method was used to calculate mRNA levels.

2.10. Western blotting analyses

Cells were disrupted in radioimmunoprecipitation assay buffer (Beyotime). Proteins were separated in an 8–12% gel. Next, proteins were transferred to polyvinylidene fluoride membranes (Millipore, Shanghai, China). The membranes were blocked with 5% non-fat milk and incubated at 4 °C with the primary antibodies for 12 h (Table 1). The corresponding secondary antibody was added, and the membranes were incubated for a further 2 h. An enhanced chemiluminescent detection reagent (Millipore, Shanghai, China) was applied to detect immunoreactive bands. A Bio-Rad XRS chemiluminescence detection system was used to measure band intensity.

2.11. Assay of ROS levels in vitro

ROS levels were assayed using a Reactive Oxygen Species Assay Kit (Beyotime). Briefly, cells were rinsed in medium without serum, and treated with 25 mM 2,' 7′-dichlorofluorescein diacetate at 37 °C for 30 min with shaking every 5 min. Finally, the cell suspension was assayed at 525 nm emission and 488 nm excitation wavelengths using a flow cytometer.

2.12. Immunofluorescence staining analysis

The protocols of Immunofluorescence staining analysis were in accordance with the previous studies [47–49]. *In vitro*, cells were cultured in a 12-well or 24-well plate. After treatment, cells were fixed and then blocked in 5% bovine serum albumin for 15–30 min. Next, they were incubated with a primary antibody at 4 °C overnight. On the following day, cells were washed with PBS and incubated with a fluorescence-conjugated secondary antibody for 2 h at romm temperature, and nuclei were stained with 4',6-diamidino-2-phenylindole for additional 5 min. *In vivo*, 5-μmm thickness was cut and mounted onto slides. After deparaffinization, subsequent process was the same as above *in vitro*. The fluorescence intensities of five random visual fields in the whole articular cavity from each group were measured by photoshop software [50].

2.13. Luciferase reporter assay

According to previous studies [51,52], a luciferase reporter construct (Nf-κb-Luc, Promega) was used to infected chondrocytes. The infected cells were treated with IL-1β (10 ng/mL) and/or HPBzyme for ~6 h. Luciferase activity was analyzed using a luciferase assay system (Promega).

Table 1
Detail of primary antibodies for Western blot analysis.

Name	Manufacturers	Product code	Dilution
MMP3	abcam	ab52915	1:1000
MMP9	proteinteck	10375-2-AP	1:1000
BAX	CST	2772T	1:1000
BCL-2	proteinteck	12789-1-AP	1:1000
COL2	abcam	ab188570	1:1000
Casepase 3	CST	9661T	1:1000
Casepase 9	CST	9508T	1:1000
COX-2	proteinteck	66351-1-Ig	1:1000
MMP13	proteinteck	18165-1-AP	1:500
iNOS	proteinteck	18985-1-AP	1:1000
Rac1	proteinteck	24072-1-AP	1:1000
p-p65	CST	3033T	1:1000
t-p65	CST	8242T	1:1000
GAPDH	proteinteck	60004-1-Ig	1:8000

2.14. In vivo evaluation

The experiments below were performed according to the guidelines of the Animal Care and Use Committee of Zhejiang Province and of the Institutional Animal Care and Use Committee of Zhejiang University. A total of 28 rats was randomly divided into four groups (seven rats per group) as follows: sham group (0.05 mL isosmotic saline solution once weekly for 4 weeks after surgery); OA group (medial meniscectomy, and 0.05 mL isosmotic saline solution once weekly for 4 weeks after surgery); low-dose HPBzyme group (medial meniscectomy and 0.05 mL HPBzyme (0.36 μg/mL) once weekly for 4 weeks after surgery); and high-dose HPBzyme group (medial meniscectomy and 0.05 mL HPBzyme (3.6 μg/mL) once weekly for 4 weeks after surgery).

3-month-old male Sprague-Dawley rats (about 200 g were anesthetized with 0.3% sodium pentobarbital (Sigma-Aldrich) intraperitoneally (30 mg/kg) [53]. The medial meniscus of the left knee was removed to develop an OA model. The surgery was performed by two senior orthopedic physicians (WZ and CY) using a medial para-patellar approach. The medial meniscus was resected using a sharp knife, and the wound was closed by suturing with 4–0 polyamide nylon. Rats in the sham group underwent the same capsulotomy and suturing without meniscectomy. After surgery, the rats received subcutaneous injections of 0.05 mg/kg buprenorphine for analgesia.

The rats were euthanized in a CO_2 chamber at 8 weeks after surgery. The knees were excised for histological analyses.

2.15. Assay of ROS levels in vivo

In accordance with a previous report [54], after treatment and euthanasia, 50 mg rat articular cartilage was collected into homogenate buffer. Next, the supernatant was incubated with ROS probe (BestBio, China) in darkness for 30 min. ROS were analyzed using a fluorescence microplate reader at a 488 nm excitation wavelength and 530 nm emission wavelength.

2.16. Histological evaluation

Samples were fixed with 4% paraformaldehyde for 48 h. Before embedding, the tissues were decalcified using 10% EDTA (Sigma) at 4 °C, twice per week for 8 weeks. Serial sections of 5 μm thickness were cut and mounted onto slides. Hematoxylin and eosin staining (H&E), and fast green and safranin O staining were carried out on consecutive tissue sections [55]. Breifly, for H&E, after deparaffinization, sections were rehydrated and then stained with hematoxylin for 30 s, rinsed in water for 120 s, eosin for 5 s, and gradient eluted with alcohol. For Safranin O and Fast green, sections after deparaffinization were also rehydrated and stained with Fast green for 5 min, rinsed for 5 min with saline solution, Safranin O for 3 min, rinsed for 5 min with saline solution again, and gradient eluted with alcohol. For histopathological evaluation of OA, the Mankin score was used. The Mankin score comprises structure (0–6 points), cellular abnormalities (0–3 points), matrix staining (0–4 points), and tidemark integrity (0–1 point) [56]. Cartilage degeneration was evaluated using the Osteoarthritis Research Society International (OARSI) scoring system [57]. Synovitis score were also applied in accordance with previous studies [58,59].

2.17. Statistical analyses

SPSS software was used for statistical analyses. Experiments were repeated at least three times, and continuous data are presented as means ± standard deviation (SD). The two-tailed Student's *t*-test was used to analyze the statistical significance of differences between two groups. A value of $P \leq 0.05$ was considered indicative of statistical significance.

3. Results and discussion

3.1. Preparation and characterization of HPBzymes

Compared with solid structure, mesoporous structure can provide a larger specific surface area and improve the contact area between catalyst and reactant, thus further improving the catalytic efficiency. HPBzymes with hollow mesoporous structure were constructed via a modified hydrothermal method (Fig. 1a). Bismuth source with PVP was added into potassium ferricyanide with PVP slowly at 30 °C, forming brownish red solution. The above solution was transferred to the oven at 80 °C for 20 h, finally achieving HPBzyme solution. The possible forming mechanism of HPBzyme was described as follow. Firstly, Bi^{3+} ions reacted with $[Fe(CN)_6]^{3-}$ to form $Bi^{3+}/[Fe(CN)_6]^{3-}$ Prussian blue analogue with unit group of Fe–CN–Bi at 30 °C. As temperature increased to 80 °C, $[Fe(CN)_6]^{3-}$ ions were reduced into $[Fe(CN)_6]^{4-}$ ions, and $[Fe(CN)_6]^{3-}$ ions ionized Fe^{3+} ions. Subsequently, the ionized Fe^{3+} ions were reduced into Fe^{2+} ions. $Bi^{3+}/[Fe(CN)_6]^{3-}$ reacted with Fe^{2+} (or $[Fe(CN)_6]^{4-}$ and $[Fe(CN)_6]^{3-}$ reacted with Fe^{2+} and Fe^{3+}, respectively) to form Prussian blue on the surface of $Bi^{3+}/[Fe(CN)_6]^{3-}$ Prussian blue analogue, finally achieving HPBzyme with hollow structure (Fig. 1a). Transmission electron microscopy (TEM) shows that HPBzyme has a distinct hollow structure and ~65 nm in size (Fig. 2a-c). The selected area electron diffraction pattern (Fig. 2d), and X-ray power diffraction pattern (Fig. 2f) indicate the good crystallinity and PB substrate. C, Fe, N, Bi, and K elements are uniformly distributed in the structure of HPBzyme (Fig. 2e). The UV–vis–NIR spectrum of HPBzyme demonstrates the characteristic absorbance peak at 721 nm (Fig. 2g), being ascribed to the electron transfer in the group of Fe–CN–Fe. The hydrodynamic diameter distribution of HPBzyme is shown in Fig. 2h; the average hydrodynamic diameter is ~78 nm. The zeta-potential of HPBzymes is about 1.85 mV (Fig. 2i). Fourier transform infrared spectroscopy shows the characteristic peak of the chemical group Fe–CN–Fe at 2085 cm^{-1} (Fig. 2j). The raman spectroscopy of HPBzyme displays a single raman peak (2150 cm^{-1}) in the raman silent region of biological samples, showing great potential in immunoassay, tumor cell imaging, and so on. The peaks of Fe element, peak of C1s-1 with binding energy of 284.33 eV, and peak of N1s-1 with binding energy of 396.98 eV demonstrated the chemical group of Fe–CN–Fe in the structure of HPBzyme. Peaks of C1s-4, C1s-3, C1s-2 and N1s-2 indicated the present of PVP modifying HPBzyme (Fig. S1). The specific surface area of the prepared HPBzyme is 105 m^2/g, much larger than that of solid Prussian blue nanoparticles (Fig. 2l). The mesoporous pore sizes of HPBzyme are 2.1 and 5.0 nm (Fig. 2m). The hollow mesoporous structure of HPBzyme is benefit for the reaction between HPBzyme and substrates in OA microenvironment.

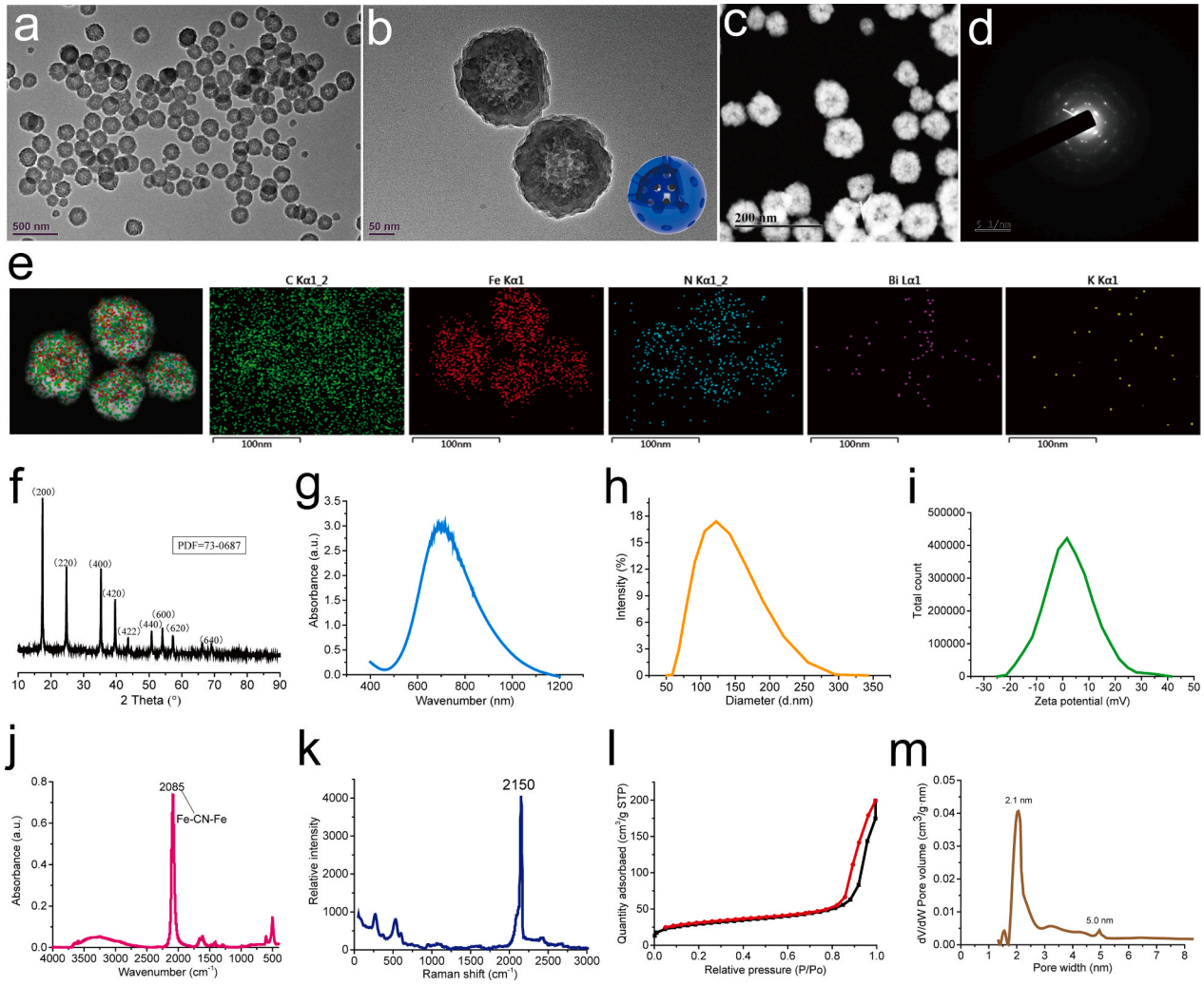

Fig. 2. Characteristics and ROS scavenging of HPBzyme. (**a-b**) TEM image of HPBzyme. (**c**) STEM image of HPBzyme. (**d**) Selected area electron diffraction of HPBzyme. (**e**) Element mapping of HPBzyme. (**f**) X-ray power diffraction of HPBzyme. (**g**) Characteristic absorbance in the near-infrared region, (**h**) hydrodynamic diameter, and (**i**) zeta potential of HPBzyme in saline. (**j**) Fourier transform infrared spectroscopy, and (**k**) raman spectroscopy of HPBzyme. (**l-m**) the specific surface area and the pore width of HPBzyme.

3.2. Catalytic activities of HPBzyme

Electron paramagnetic resonance was adopted to investigate the catalytic activity of HPBzyme. ·OH, ·OOH, and H_2O_2 were selected as ROS models. TiO_2 (P25) can generate ·OH under ultraviolet light irradiation. 5-tert-Butoxycarbonyl-5-methyl-1-pyrroline-N-oxide (BMPO) was used as a free radical spin trapping reagent. The four characteristic peaks of BMPO/·OH (1:2:2:1) were observed in the electron spin resonance (ESR) spectra of a TiO_2/UV system without HPBzyme (Fig. 3a-b). HPBzymes diminished the signal intensity of BMPO/·OH in a concentration- and time-dependent manner (Fig. 3c-d), demonstrating the good ·OH scavenging property of HPBzymes. The xanthine/xanthine oxidase (XO/XOD) system generating ·OOH was selected to explore the SOD-like activity of HPBzyme. The signal intensities of the four characteristic peaks of BMPO/·OOH (1:1:1:1) in the ESR spectra decreased with increasing of HPBzyme concentration and increasing reaction time (Fig. 3c-d), showing the good SOD-like activity of HPBzymes. The characteristic signal of O_2 was tested in the H_2O_2 with HPBzymes via ESR (Fig. 3e-f), showing the catalase-like activity of HPBzyme. HPBzyme converted harmful ROS including ·OH, ·OOH, and H_2O_2 into harmless H_2O and O_2, reducing overproducted ROS levels to normal levels (Fig. 3g). The catalytic activity of HPBzyme on ·OH, ·OOH, and H_2O_2 showed the potential in the remodeling OA microenvironment.

3.3. HPBzyme attenuates IL-1β-induced inflammation in human chondrocytes

IL-1β blocks the synthesis of ECM components by chondrocytes and interferes with the synthesis of key structural proteins, such as type-II collagen (COL2) and aggrecan [60]. When chondrocytes are stimulated by IL-1β, they age rapidly or undergo apoptosis [61]. IL-1β inhibits cartilage repair and accelerates cartilage degeneration through enzymes, thereby directly affecting chondrocytes [62]. Therefore, IL-1β has been used to induce OA microenvironment *in vitro* [63,64]. To facilitate translation into clinical practice, we used IL-1β to induce inflammation in human chondrocyte to evaluate the inhibitory effects of HPBzyme on OA inflammation. The effects of HPBzyme at various concentrations (ranging from 0 to 200 μg/mL) on human chondrocytes proliferation were evaluated using a CCK-8 assay; no cytotoxicity effects were detected (0–72 μg/mL) over 24 h (Fig. S2). In subsequent experiments, 0.36 and 36 μg/mL HPBzyme were defined as low and high dose. IL-1β induces the secretion by chondrocytes of cytokines such as IL-6, iNOS and COX-2, leading to the aggravation of OA [65,66]. Therefore, we used polymerase chain reaction (PCR) to assay IL-6, COX-2 and iNOS expression in chondrocytes culture supernatant to evaluate the anti-inflammatory effects of HPBzyme. HPBzyme was incubated with human chondrocytes for 2 h, followed by IL-1β (10 ng/mL) for 24 h. In chondrocytes, IL-1β stimulates the synthesis of IL-6 and other cytokines in an autocrine manner

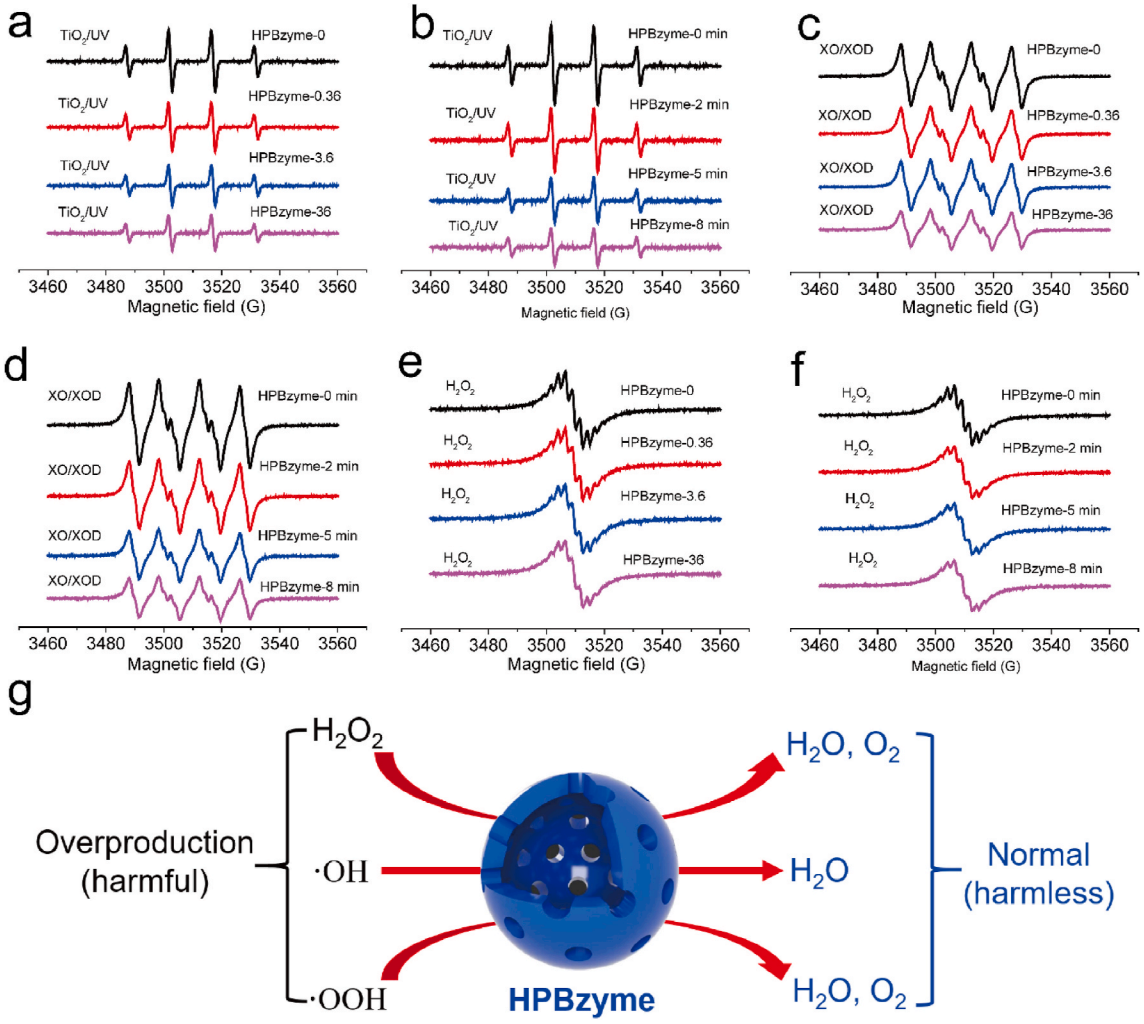

Fig. 3. (**a-b**) Scavenging by HPBzyme of •OH generated by a TiO_2/UV system. (**c-d**) Scavenging by HPBzyme of •OOH. Effect of HPBzyme on the generation of O_2 from H_2O_2 as determined by ESR oximetry. (**e-f**) O_2 generation from H_2O_2 degradation catalyzed by HPBzyme was measured in a closed chamber containing 0.1 mM CTPO, 25 mM H_2O_2, and HPBzyme in PBS (Ph 7.4). (**g**) Overproduction of •OH, •OOH, and H_2O_2 was reduced by HPBzyme.

[67]. IL-6 influences subchondral bone by enhancing osteoclast formation, leading to bone absorption, and shows a synergistic effect with IL-1β and TNF-α [63,67]. The IL-6 level in chondrocyte culture supernatant was significantly increased by IL-1β [66,68]. When human chondrocytes were exposed to HPBzyme (0.36 μg/mL and 36 μg/mL) before IL-1β stimulation, the level of IL-6 in supernatant decreased four and six-fold, respectively (Fig. S3). In addition, HPBzyme reduced the IL-6 mRNA levels in chondrocytes as determined by PCR (Fig. 4a). COX-2 is a proinflammatory cytokine that plays an important role in proteoglycan synthesis, matrix degradation, and chondrocyte survival [69]. iNOS stimulates NO synthesis by chondrocytes. An increase in the NO level leads to chondrocyte injury by upregulating the activity of MMPs and preventing the biosynthesis of aggrecan and COL2 [70,71]. HPBzyme pretreatment significantly downregulated the increased COX2 and iNOS mRNA levels induced by IL-1β (Fig. 4b-c). In addition, the iNOS and COX-2 protein levels were consistent with their mRNA levels (Fig. 4d-f). Immunofluorescence analyses showed that HPBzyme reduced the COX-2 protein level (Fig. 4g). HPBzyme reduced the inflammatory cytokines of OA microenvironment efficiently, even with low concentration of 0.36 μg/mL.

3.4. *HPBzyme inhibits ECM degradation and human chondrocyte apoptosis via remodeling IL-1β-induced microenvironment in human chondrocytes*

Chondrocyte apoptosis and ECM degradation are the most important characteristic pathological changes in OA [22]. MMP-3 degrades aggrecan, adhesin, collagens and fibrin in chondrocytes, and activates other MMPs. MMP-9 activates collagenase, destroys the collagen network structure, and degrades mainly denatured interstitial collagen and basement membrane collagen [72]. MMP-13 is a major structural component of cartilage and degrades COL2 [17]. COL2 and aggrecan are the main components of cartilage; their levels can be used as indicators of the degree of cartilage degeneration. Such degeneration suppresses ECM regeneration, leading to cartilage degradation. the mRNA level of MMP-3, and MMP-13 increases significantly and accelerates the degradation of COL2 and aggrecan compared to the control group after IL-1β stimulation (Fig. 5a-d). However, HPBzyme significantly inhibited the increased expression of MMP-3 and -13 in human chondrocytes stimulated by IL-1β, delaying the degradation of aggrecan and COL2, and thus slowing the development of OA (Fig. 5a-d). The results of Western blotting of chondrocyte proteins were consistent with those of qRT-PCR (Fig. 5e-g). Immunofluorescence analyses also showed that HPBzyme significantly downregulated IL-1β-induced MMP-9 release (Fig.s 5j). In addition, IL-1β stimulation resulted in marked loss of safranine O staining in human chondrocytes (Fig. 5k). However, HPBzyme significantly reduced the IL-1β-induced loss of safranin O staining in human chondrocytes (Fig. 5k). Similarly, HPBzyme delayed IL-1β-mediated downregulation of the levels of GAGs in chondrocytes (Fig. S5). Apoptosis of chondrocytes is related to cartilage morphology, function, and OA. Caspase-3 and -9 promote chondrocyte apoptosis [13]. Nuclear factor-erythroid 2-related factor 2 prevents chondrocyte apoptosis by

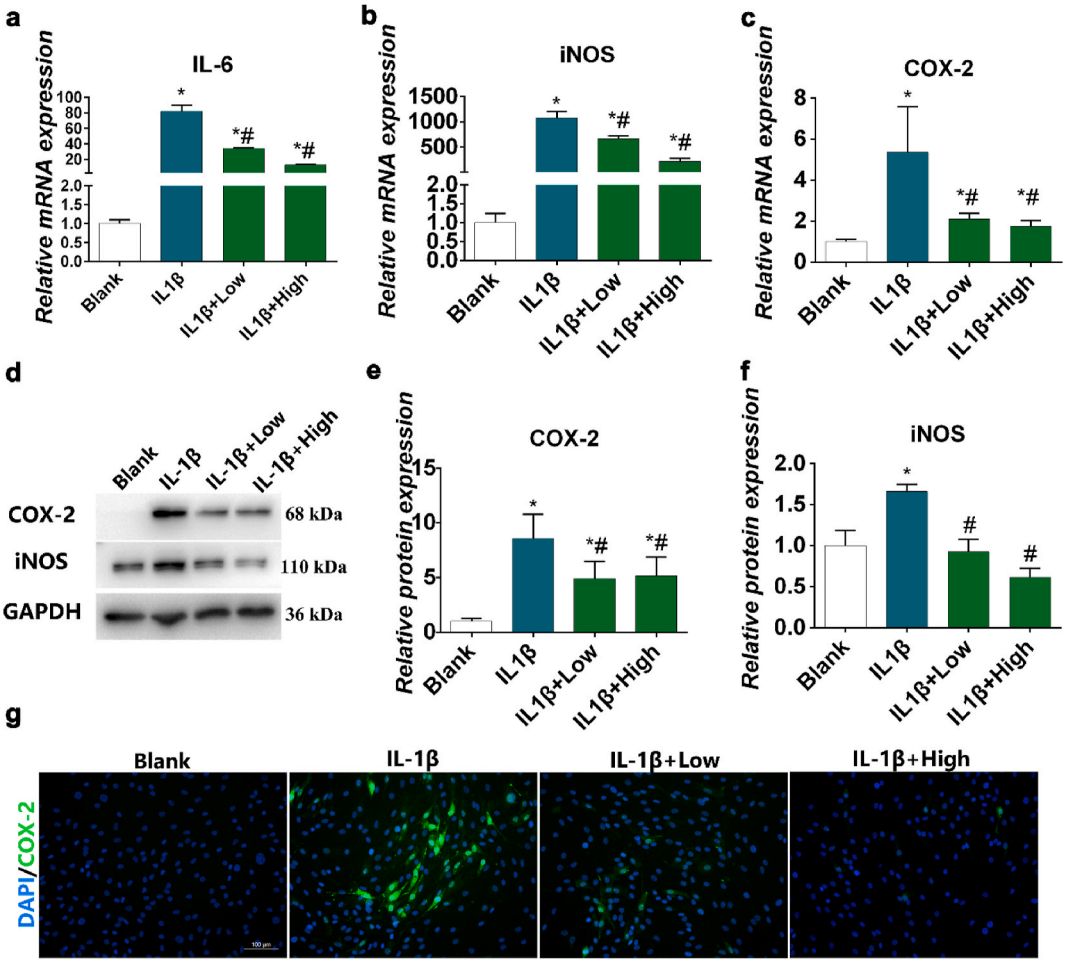

Fig. 4. HPBzyme attenuates IL-1β-induced inflammation in chondrocytes. 0.36 and 36 μg/mL HPBzyme were defined as low and high dose. Effects of HPBzyme on the (**a**) IL-6, (**b**) iNOS, and (**c**) COX-2 mRNA level in chondrocytes as determined by qRT-PCR. (**d-f**) Effects of HPBzyme on the COX-2 and iNOS protein levels as determined by Western blotting analyses after IL-1β stimulation. Protein levels were normalized to that of GAPDH. (**g**) Effect of HPBzyme on COX-2 in chondrocytes as determined by immunofluorescence; magnification, × 200, bar, 100 μm. Data are means ± standard deviation (SD), n = 3. *P < 0.05 vs. blank group (chondrocytes without HPBzyme and IL-1β), $^{\#}P < 0.05$ vs. IL-1β group (chondrocytes with only IL-1β stimulation).

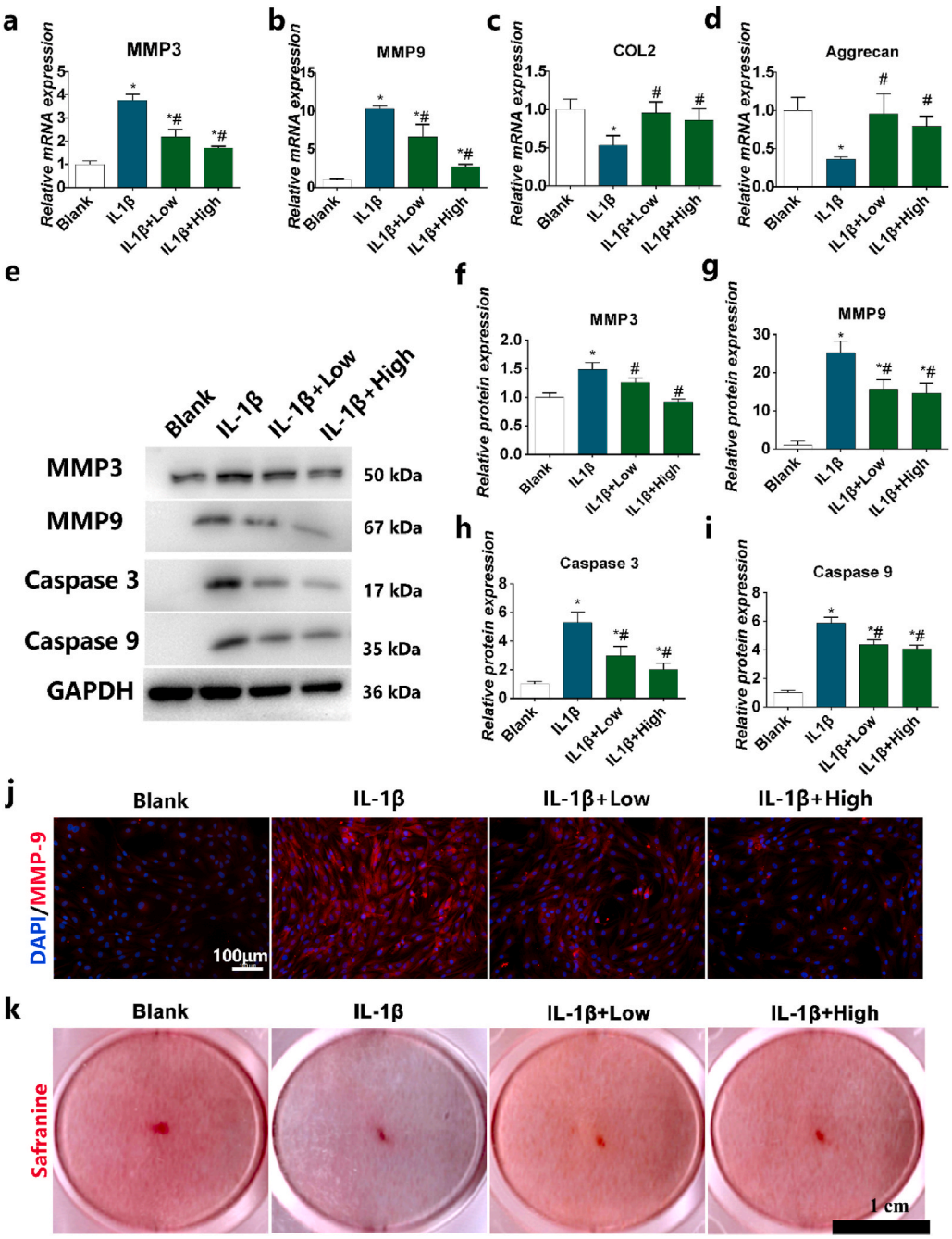

Fig. 5. HPBzyme inhibits ECM degradation and apoptosis of chondrocytes. (**a**) MMP3 mRNA level as determined by qRT-PCR. (**b**) MMP13 mRNA level as determined by qRT-PCR. (**c**) COL2 mRNA level as determined by qRT-PCR. (**d**) Aggrecan mRNA level as determined by qRT-PCR. (**e-i**) Effects of HPBzyme on the MMP-3 and -9, Caspase-3 and -9 protein levels after IL-1β induction as determined by Western blotting analyses. Protein levels were normalized to that of GAPDH. (**j**) Immunofluorescence staining of the effects of HPBzyme on the MMP-9 level after IL-1β stimulation. magnification, × 200, Bar, 100 μm. (**k**) Effect of HPBzyme on proteoglycans in chondrocytes after IL-1β stimulation as determined by safranin O staining, Bar, 1 cm. Data are means ± SD, n = 3. $^{*}P < 0.05$ vs. blank group (chondrocytes without HPBzyme and IL-1β), $^{\#}P < 0.05$ vs. IL-1β group (chondrocytes with only IL-1β stimulation).

suppressing the levels of caspase-3 and ROS [25]. IL-1β induced the expression of Caspase-3 and -9, indicating the apoptosis of human chondrocytes. However, the prepared HPBzyme significantly reduced the caspase-3 and -9 levels in human chondrocytes stimulated by IL-1β (Fig. 5e, and 5h-5i). Compared to the blank control group, the apoptosis rate of chondrocytes was increased significantly by H_2O_2 after 24 h (Fig. 6a-b). However, HPBzyme significantly reduced the H_2O_2-induced apoptosis of human chondrocytes (Fig. 6a-b).

3.5. *HPBzyme remodels IL-1β-induced microenvironment in human chondrocytes via attenuating ROS and Rac1-NF-κB signaling pathway*

The signaling pathways involved in the pathogenesis of OA are Hedgehog, Wnt, and SDF-1/CXCR4 [28,73,74]. Intracellular signaling pathways are independent and interrelated, forming a complex network. Oxidative stress and ROS are closely related to the pathogenesis of OA, and result in MMPs production, ECM degradation, joint inflammation and chondrocyte apoptosis [12,19,24]. Excessive ROS can cause DNA damage in OA cartilage [24]. Moreover, ROS and ras-related C3 botulinum toxin substrate 1 (Rac1)–NF–κB signaling plays a critical role in accelerating OA [75]. Next, we investigated the signaling pathway by which HPBzyme remodels OA microenvironment via influencing inflammation, ROS generation, ECM degradation, and apoptosis. ROS regulate cartilage metabolism, chondrocyte apoptosis, ECM synthesis and decomposition, and cytokine production [18]. The balance of ROS and antioxidants is related to the occurrence, development and progress of OA. Excessive ROS participate in various signal pathways activated by injury or cytokines, amplify inflammation and accelerate chondrocyte catabolism and apoptosis [25]. Hydrogen peroxide and inflammation induce excessive ROS production in chondrocytes [26]. HPBzyme

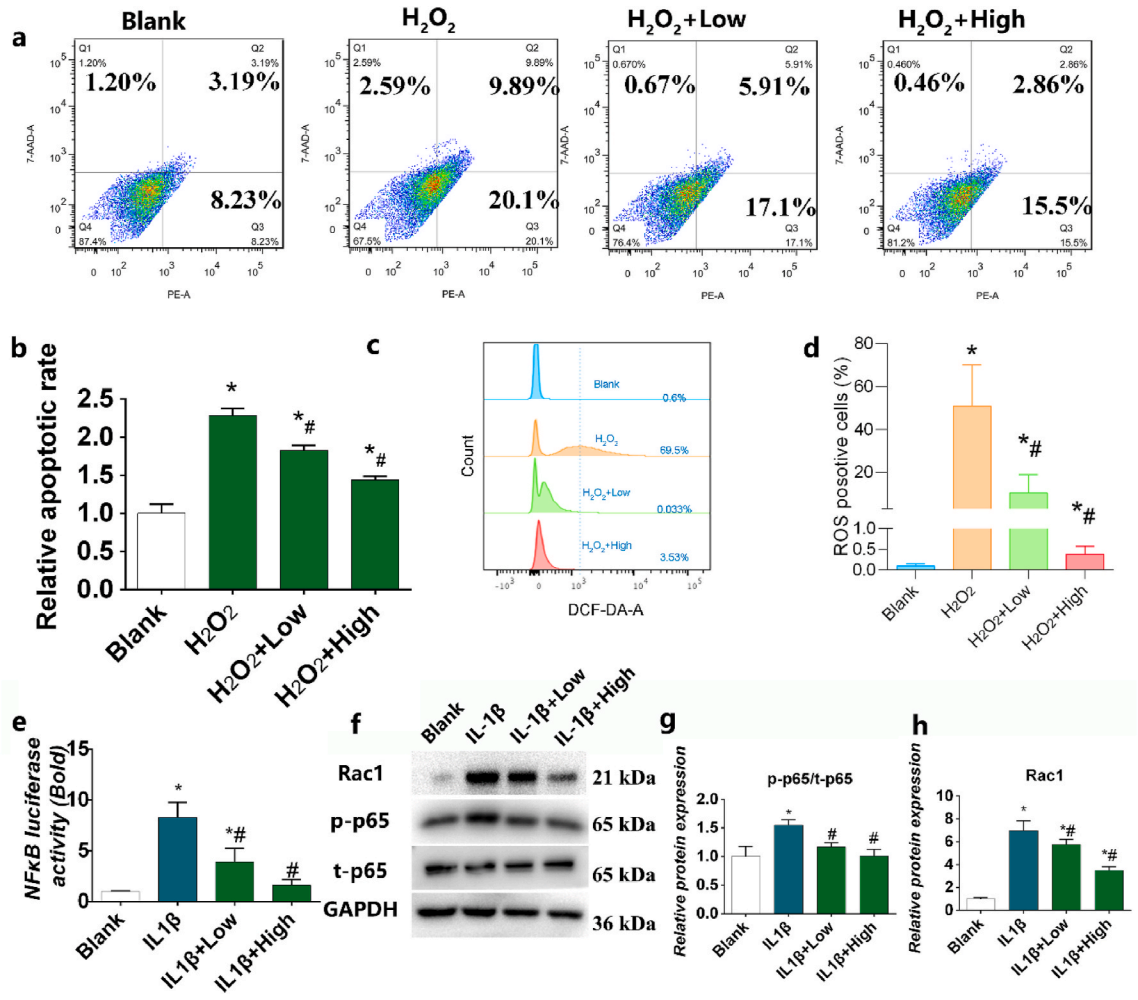

Fig. 6. HPBzyme suppresses the Rac1-ROS-NFκB signaling pathway. ((**a-b**) Effect of HPBzyme on chondrocyte apoptosis after H_2O_2 treatment. (c–d) Effect of HPBzyme on ROS levels after IL-1β treatment as determined by flow cytometry. (**e**) Effect of HPBzyme on NF-κB signaling after IL-1β treatment as determined by luciferase reporter assay. (**f**) Effect of HPBzyme on the Rac1, p-p65, and t-p65 protein levels after IL-1β induction as determined by Western blotting analyses. Protein levels were normalized to that of GAPDH. Data are means ± SD, n = 3. $^{*}P < 0.05$ vs. blank group (chondrocytes without HPBzyme and IL-1β), $^{\#}P < 0.05$ vs. IL-1β group (chondrocytes with only IL-1β stimulation).

significantly reduced the levels of ROS in H_2O_2-induced human chondrocytes (Fig. 6c-d), amplifying inflammation and accelerating chondrocyte catabolism and apoptosis. NF-κB is an important target of ROS in the inflammatory response, catabolism, survival, and apoptosis. The Rac1and ROS activate NF-κB translation in chondrocytes [75,76]. As a second messenger, excess ROS upregulate NF-κB, aggravating the inflammatory response and increasing MMP levels and apoptosis [18]. The inactive NF-κB dimer binds to inhibitor of NF-κB (IκB) in the cytoplasm. However, in the active state, IκB protein in the cytoplasm is phosphorylated and degraded after chemical or mechanical stimulation. Next, NF-κB dimer is released and translocated to the nucleus, inducing target gene transcription [77]. IL-1β significantly upregulated NF-κB, promoted p65 nuclear translocation, and activated Rac1 (Fig. 6e-h). Furthermore, Western blotting analyses showed that IL-1β-induced increasing p-p65, and t-p65 protein levels could be inhibited by HPBzyme (Fig. 6f-h). HPBzyme remodels IL-1β-induced microenvironment in human chondrocytes via attenuating ROS, Rac1and NF-κB signaling pathway.

3.6. HPBzyme delayed the progression of OA in vivo

To investigate the effects of HPBzyme on chondrocytes, a rat model of traumatic OA was established by medial meniscectomy. In the sham group, the articular cartilage surface was smooth and complete; there is no decrease in safranine O staining; the cartilage structure and tidal line were intact; the surface and middle layers comprised flat and round chondrocytes, respectively, and the deep and calcified layers contained proliferative chondrocytes with high proteoglycan content (Fig. 7a). In the OA group, decreased safranin O staining, joint space narrowing, cartilage damage, osteophyte formation, and subchondral bone sclerosis were observed (Fig. 7a). The surface cartilage became swollen and round; the number of chondrocytes decreased significantly; chondrocytes clustered; cells were arranged disorderly and irregularly; cracks were observed; there were multiple tidal lines and irregularities; and the proteoglycan content decreased (Fig. 7a). In the HPBzyme group, the number of chondrocytes and the aggrecan level increased (Fig. 7a). In addition, chondrocytes were arranged more regularly than those in the OA group (Fig. 7a). The effects of HPBzyme showed dose-dependent profile (Fig. 7a). Evaluation of Mankin's score [56,78] showed that HPBzyme significantly decreased the severity of OA of the knee joint compared to the OA group, indicating that HPBzyme delayed the progression of OA (Fig. 7b). The OARSI score was decreased by HPBzyme compared to the OA group (Fig. 7c). Immunofluorescence analysis showed that compared to the OA group, the expression of iNOS and COX-2 in cartilage treated with HPBzyme was significantly down-regulated the microenvironment of chondrocytes (Fig. 7d–g). We also

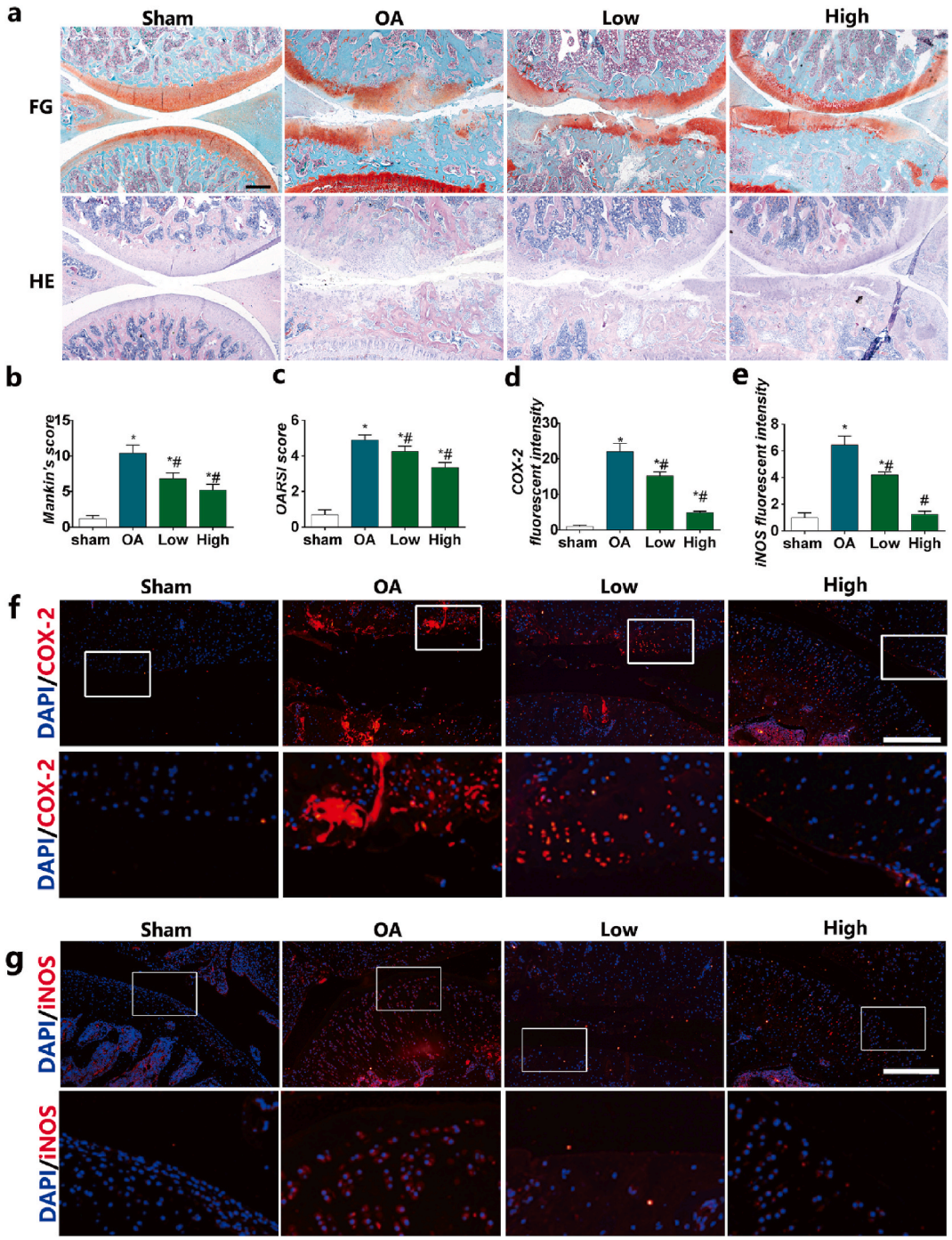

Fig. 7. HPBzyme delays the progression of osteoarthritis *in vivo*. (**a**) Histologic analyses of osteoarthritis. HE, hematoxylin and eosin staining; FG, safranin O and fast green staining; magnification, × 40; Bar, 500 μm. (**b**) Mankin's score of OA. (**c**) OARSI score of cartilage degeneration. (**d-g**) Effect of HPBzyme on the protein levels of COX-2 and iNOS *in vivo* by IF. Bar, 100 μm. Data are means ± SD, n = 3. $^{*}P < 0.05$ vs. sham group (rat knee joint without HPBzyme and meniscectomy), $^{\#}P < 0.05$ vs. OA group (rat knee joint with only meniscectomy).

evaluated markers of OA, including inflammatory factors, catabolic enzymes, ECM and chondrocyte apoptosis (Fig. 8). The effects of HPBzyme on the BAX, iNOS, Caspase 3, MMP13, COL2, Rac1, and p-p65/t-p65 protein levels were determined by Western blotting *in vivo* (Fig. 8). As shown in Fig. 8a-b, the represented inflammatory cytokine iNOS were investigated *in vivo*. HPBzyme with low concentration reduced the expression of iNOS (Fig. 8a-b), being consistent with the results *in vitro*. HPBzymes significantly reversed the increased BAX, and caspase-3, demonstrating the inhibiting effect of HPBzyme on cell apoptosis in the treatment of OA. The increased expression of COL2 were observed in the treatment with HPBzyme groups, indicating the inhibition of ECM degradation *in vivo*. HPBzyme markedly decreased the ROS levels *in vivo* (Fig. 8i). Furthermore, Rac1, and p-p65/t-p65 protein levels associated with OA progression in rat articular cartilage were also tested (Fig. 8a, g, 8h). According to previous studies [58,59], H&E staining showed a decrease in lining cells and a lower density of resident cells in the synovium in the group treated with HPBzymes as compared to the OA group; The density of the synovial stroma was decreased in high dose HPBzymes group. The synovitis score of the synovium were significant downregulated after the treatment of HPBzymes (Fig. S5).

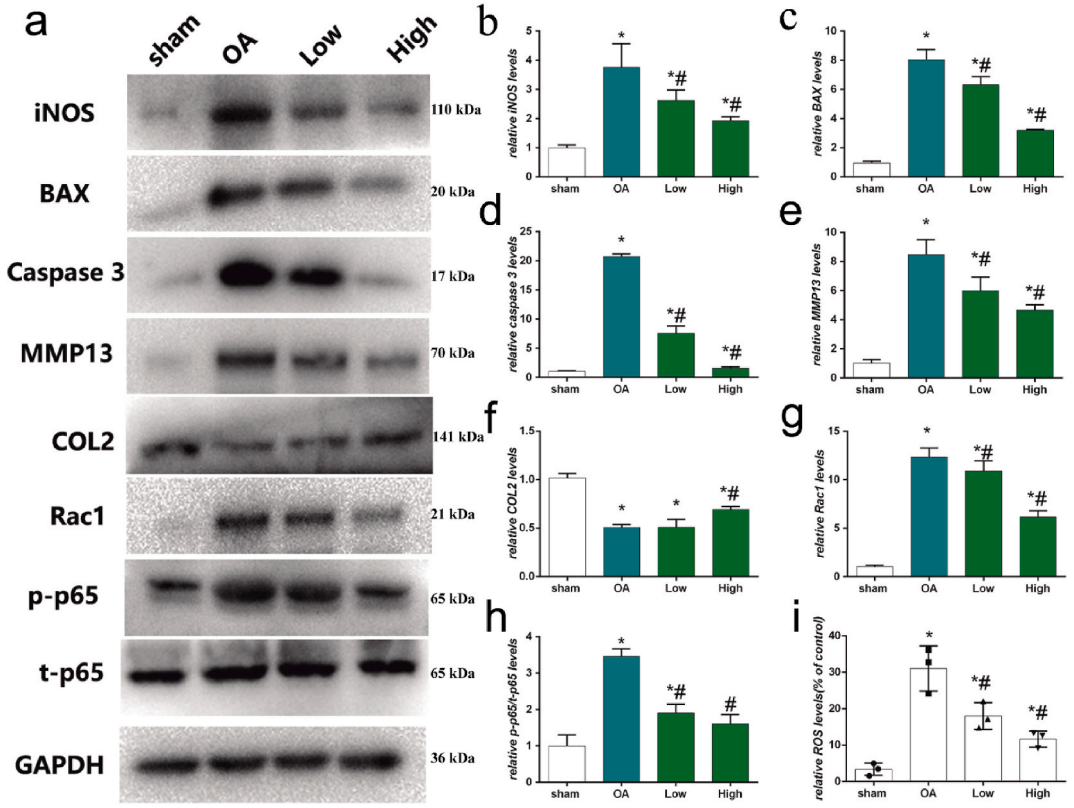

Fig. 8. HPBzyme delays the progression of osteoarthritis *in vivo*. (**a-h**) Effect of HPBzyme on the BAX, iNOS, caspase 3, MMP13, COL2, Rac1, p-p65, and t-p65 protein levels as determined by Western blotting analyses *in vivo*. Protein levels were normalized to that of GAPDH. (**i**) The effects of HPBzymes on ROS levels were determined by flow cytometer analysis *in vivo*. Data are means ± SD, n = 3. $^{*}P < 0.05$ vs. sham group (rat knee joint without HPBzyme and meniscectomy), $^{\#}P < 0.05$ vs. OA group (rat knee joint with only meniscectomy).

The above results indicated that HPBzyme remodels OA microenvironment, and thus delay the progression of OA *in vivo* via attenuating ROS and Rac1-NF-κB signaling pathway.

4. Conclusion

In summary, HPBzymes remodeled the microenvironment of OA for attenuating inflammation, cartilage ECM degradation and cells apoptosis, increasing the expression of COL2 and aggrecan, to protect articular cartilage, and delay the development of OA via the ROS and Rac1-NF-κB signaling pathway. Nanozyme-mediated microenvironment remodeling is an effective strategy for the treatment of OA, and possibly also for other ROS/inflammation-related diseases. We used the FDA-approved components of simple composition and that lack side effects within the effective dose range. Importantly, the intrinsic bioactivities of HPBzymes mediated their therapeutic effect. This study is a preliminary study provided a novel and effective option for the treatment of OA and suggest a consequet direction for the translation of nanozyme-therapies to the clinic. No cytokine or signaling pathway fully explains the pathogenesis of OA. However, our findings provide insight into the pathogenesis, prevention, and treatment of OA, as well as ROS-mediated bone diseases, including osteoporosis, bone erosion, bone defect. The hollow structure, size and particle size of HPBzymes can be controlled. HPBzymes acting as a drug carrier, are easy to combine with other therapies and play a greater role in treatment.

CRediT authorship contribution statement

Weiduo Hou: Methodology, Software, Validation, Investigation. **Chenyi Ye:** Methodology, Data curation, Investigation. **Mo Chen:** Methodology, Investigation. **Wei Gao:** Investigation, Resources. **Xue Xie:** Validation. **Jianrong Wu:** Formal analysis. **Kai Zhang:** Writing - review & editing. **Wei Zhang:** Conceptualization, Methodology, Writing - original draft. **Yuanyi Zheng:** Conceptualization, Writing - review & editing, Visualization, Funding acquisition. **Xiaojun Cai:** Conceptualization, Investigation, Writing - original draft, Writing - review & editing, Supervision, Project administration, Funding acquisition.

Declaration of competing interest

The authors declare that they have no known competing financial interests or personal relationships that could have appeared to influence the work reported in this paper.

Acknowledgements

This study was supported by the National Natural Science Foundation of China (no. 81801822), Shanghai S&T Major project (2018SHZDZX05), NSFC Key Projects of International Cooperation and Exchanges (81720108023), Shanghai Collaborative Innovation Center for Translational Medicine (no. TM201724), Natural Science Foundation of Shanghai (18ZR1429300), Interdisciplinary Program of Shanghai Jiao Tong University (no. YG2017QN20).

Appendix A. Supplementary data

Supplementary data to this article can be found online at https://doi.org/10.1016/j.bioactmat.2021.01.016.

References

[1] B.S. Ferket, Z. Feldman, J. Zhou, E.H. Oei, S.M. Bierma-Zeinstra, M. Mazumdar, Impact of total knee replacement practice: cost effectiveness analysis of data from the Osteoarthritis Initiative, BMJ 356 (2017) j1131.

[2] D.J. Hunter, S. Bierma-Zeinstra, Osteoarthritis, Lancet 393 (2019) 1745–1759.
[3] P. Castrogiovanni, M. Di Rosa, S. Ravalli, A. Castorina, C. Guglielmino, R. Imbesi, M. Vecchio, F. Drago, M.A. Szychlinska, G. Musumeci, Moderate physical activity as a prevention method for knee osteoarthritis and the role of synoviocytes as biological key, Int. J. Mol. Sci. 20 (2019).
[4] M.A. Szychlinska, R. Imbesi, P. Castrogiovanni, C. Guglielmino, S. Ravalli, M. Di Rosa, G. Musumeci, Assessment of vitamin D supplementation on articular cartilage morphology in a young healthy sedentary rat model, Nutrients 11 (2019).
[5] M. Kloppenburg, F.P. Kroon, F.J. Blanco, M. Doherty, K.S. Dziedzic, E. Greibrokk, I. K. Haugen, G. Herrero-Beaumont, H. Jonsson, I. Kjeken, E. Maheu, R. Ramonda, M. J. Ritt, W. Smeets, J.S. Smolen, T.A. Stamm, Z. Szekanecz, R. Wittoek, L. Carmona, Update of the EULAR recommendations for the management of hand osteoarthritis, Ann. Rheum. Dis. 78 (2018) 16–24, 2019.
[6] D. Gregori, G. Giacovelli, C. Minto, B. Barbetta, F. Gualtieri, D. Azzolina, P. Vaghi, L.C. Rovati, Association of pharmacological treatments with long-term pain control in patients with knee osteoarthritis: a systematic review and meta-analysis, J. Am. Med. Assoc. 320 (2018) 2564–2579.
[7] T. Grosser, E. Ricciotti, G.A. FitzGerald, The cardiovascular pharmacology of nonsteroidal anti-inflammatory drugs, Trends Pharmacol. Sci. 38 (2017) 733–748.
[8] S. Castorina, C. Guglielmino, P. Castrogiovanni, M.A. Szychlinska, F. Ioppolo, P. Massimino, P. Leonardi, C. Maci, M. Iannuzzi, A. Di Giunta, G. Musumeci, Clinical evidence of traditional vs fast track recovery methodologies after total arthroplasty for osteoarthritic knee treatment. A retrospective observational study, Muscles, ligaments and tendons journal 7 (2017) 504–513.
[9] M. Pollock, L. Somerville, A. Firth, B. Lanting, Outpatient total hip arthroplasty, total knee arthroplasty, and unicompartmental knee arthroplasty: a systematic review of the literature, JBJS Rev 4 (2016).
[10] D. Hunter, S. Bierma-Zeinstra, Osteoarthritis, Lancet 393 (2019) 1745–1759.
[11] E.M. Roos, N.K. Arden, Strategies for the prevention of knee osteoarthritis, Nat. Rev. Rheumatol. 12 (2016) 92–101.
[12] N. Ahmad, M.Y. Ansari, T.M. Haqqi, Role of iNOS in osteoarthritis: pathological and therapeutic aspects, J. Cell. Physiol. 235 (2020) 6366–6376.
[13] H.S. Hwang, H.A. Kim, Chondrocyte apoptosis in the pathogenesis of osteoarthritis, Int. J. Mol. Sci. 16 (2015) 26035–26054.
[14] D.J. Saxby, D.G. Lloyd, Osteoarthritis year in review 2016: mechanics, Osteoarthritis Cartilage 25 (2017) 190–198.
[15] E. Stocco, S. Barbon, M. Piccione, E. Belluzzi, L. Petrelli, A. Pozzuoli, R. Ramonda, M. Rossato, M. Favero, P. Ruggieri, A. Porzionato, R. Di Liddo, R. De Caro, V. Macchi, Infrapatellar fat pad stem cells responsiveness to microenvironment in osteoarthritis: from morphology to function, Front Cell Dev Biol 7 (2019) 323.
[16] A. Latourte, C. Cherifi, J. Maillet, H.K. Ea, W. Bouaziz, T. Funck-Brentano, M. Cohen-Solal, E. Hay, P. Richette, Systemic inhibition of IL-6/Stat3 signalling protects against experimental osteoarthritis, Ann. Rheum. Dis. 76 (2017) 748–755.
[17] H. Li, D. Wang, Y. Yuan, J. Min, New insights on the MMP-13 regulatory network in the pathogenesis of early osteoarthritis, Arthritis Res. Ther. 19 (2017) 248.
[18] P. Lepetsos, A.G. Papavassiliou, ROS/oxidative stress signaling in osteoarthritis, Biochim. Biophys. Acta 1862 (2016) 576–591.
[19] P. Lepetsos, K.A. Papavassiliou, A.G. Papavassiliou, Redox and NF-kappaB signaling in osteoarthritis, Free Radic. Biol. Med. 132 (2019) 90–100.
[20] F.J. Blanco, I. Rego, C. Ruiz-Romero, The role of mitochondria in osteoarthritis, Nat. Rev. Rheumatol. 7 (2011) 161–169.
[21] M.J. Lammi, J. Häyrinen, A. Mahonen, Proteomic analysis of cartilage- and bone-associated samples, Electrophoresis 27 (2006) 2687–2701.
[22] S. S, Y. W, J. C, Z. X, K. H, G. W, Y. Y, W. N, Z. C, P. S, Y. M, S. F, CircSERPINE2 protects against osteoarthritis by targeting miR-1271 and ETS-related gene, Ann. Rheum. Dis. 78 (2019) 826–836.
[23] G. Musumeci, M. Carnazza, C. Loreto, R. Leonardi, C. Loreto, β-Defensin-4 (HBD-4) is expressed in chondrocytes derived from normal and osteoarthritic cartilage encapsulated in PEGDA scaffold, Acta Histochem. 114 (2012) 805–812.
[24] C.M. Davies, F. Guilak, J.B. Weinberg, B. Fermor, Reactive nitrogen and oxygen species in interleukin-1-mediated DNA damage associated with osteoarthritis, Osteoarthritis Cartilage 16 (2008) 624–630.
[25] N.M. Khan, I. Ahmad, T.M. Haqqi, Nrf2/ARE pathway attenuates oxidative and apoptotic response in human osteoarthritis chondrocytes by activating ERK1/2/ELK1-P70S6K-P90RSK signaling axis, Free Radic. Biol. Med. 116 (2018) 159–171.
[26] A. H, K. Sk, M.T. J, R. D, A. S-Z, M. S, R. RJ, H. G, S. M, Apoptosis signaling pathways in osteoarthritis and possible protective role of melatonin, J. Pineal Res. 61 (2016) 411–425.
[27] J. Kim, H.Y. Kim, S.Y. Song, S.H. Go, H.S. Sohn, S. Baik, M. Soh, K. Kim, D. Kim, H. C. Kim, N. Lee, B.S. Kim, T. Hyeon, Synergistic oxygen generation and reactive oxygen species scavenging by manganese ferrite/ceria Co-decorated nanoparticles for rheumatoid arthritis treatment, ACS Nano 13 (2019) 3206–3217.
[28] C.R. Scanzello, Chemokines and inflammation in osteoarthritis: insights from patients and animal models, J. Orthop. Res. 35 (2017) 735–739.
[29] Z. Wang, R. Zhang, X. Yan, K. Fan, Structure and activity of nanozymes: inspirations for de novo design of nanozymes, Mater. Today 41 (2020) 81–119.
[30] K. Fan, J. Xi, L. Fan, P. Wang, C. Zhu, Y. Tang, X. Xu, M. Liang, B. Jiang, X. Yan, L. Gao, In vivo guiding nitrogen-doped carbon nanozyme for tumor catalytic therapy, Nat. Commun. 9 (2018) 1440.
[31] Q. Liang, J. Xi, X.J. Gao, R. Zhang, Y. Yang, X. Gao, X. Yan, L. Gao, K. Fan, A metal-free nanozyme-activated prodrug strategy for targeted tumor catalytic therapy, Nano Today 35 (2020), 100935.
[32] H. Wang, K. Wan, X. Shi, Recent advances in nanozyme research, Adv. Mater. 31 (2019), 1805368.
[33] J. Xi, R. Zhang, L. Wang, W. Xu, Q. Liang, J. Li, J. Jiang, Y. Yang, X. Yan, K. Fan, L. Gao, A nanozyme-based artificial peroxisome ameliorates hyperuricemia and ischemic stroke, Adv. Funct. Mater. (2020), 2007130.
[34] Y. Liu, Y. Cheng, H. Zhang, M. Zhou, Y. Yu, S. Lin, B. Jiang, X. Zhao, L. Miao, C. Wei, Q. Liu, Y. Lin, Y. Du, C. Butch, H. Wei, Integrated cascade nanozyme catalyzes in vivo ROS scavenging for anti-inflammatory therapy, Science advances 6 (2020), eabb2695.
[35] A. Mohammad, P.J. Faustino, M.A. Khan, Y. Yang, Long-term stability study of Prussian blue - a quality assessment of water content and thallium binding, Int. J. Pharm. 477 (2014) 122–127.
[36] J. Long, Y. Guari, C. Guerin, J. Larionova, Prussian blue type nanoparticles for biomedical applications, Dalton Trans. 45 (2016) 17581–17587.
[37] Z. Qin, Y. Li, N. Gu, Progress in applications of prussian blue nanoparticles in biomedicine, Adv Healthc Mater 7 (2018), e1800347.
[38] G. Dacarro, A. Taglietti, P. Pallavicini, Prussian blue nanoparticles as a versatile photothermal tool, Molecules 23 (2018).
[39] J. Zhao, X. Cai, W. Gao, L. Zhang, D. Zou, Y. Zheng, Z. Li, H. Chen, Prussian blue nanozyme with multienzyme activity reduces colitis in mice, ACS Appl. Mater. Interfaces 10 (2018) 26108–26117.
[40] L. Sun, Q. Li, M. Hou, Y. Gao, R. Yang, L. Zhang, Z. Xu, Y. Kang, P. Xue, Light-activatable Chlorin e6 (Ce6)-imbedded erythrocyte membrane vesicles camouflaged Prussian blue nanoparticles for synergistic photothermal and photodynamic therapies of cancer, Biomaterials science 6 (2018) 2881–2895.
[41] W. Zhang, S. Hu, J.J. Yin, W. He, W. Lu, M. Ma, N. Gu, Y. Zhang, Prussian blue nanoparticles as multienzyme mimetics and reactive oxygen species scavengers, J. Am. Chem. Soc. 138 (2016) 5860–5865.
[42] C.R. Patra, Prussian blue nanoparticles and their analogues for application to cancer theranostics, Nanomedicine 11 (2016) 569–572.
[43] J. Fan, J.J. Yin, B. Ning, X. Wu, Y. Hu, M. Ferrari, G.J. Anderson, J. Wei, Y. Zhao, G. Nie, Direct evidence for catalase and peroxidase activities of ferritin-platinum nanoparticles, Biomaterials 32 (2011) 1611–1618.
[44] F. H, A. H, H. MF, Apoptosis in normal and osteoarthritic human articular cartilage, Ann. Rheum. Dis. 59 (2000) 959–965.
[45] N.M. Khan, M.Y. Ansari, T.M. Haqqi, Sucrose, but not glucose, blocks IL1-beta-induced inflammatory response in human chondrocytes by inducing autophagy via AKT/mTOR pathway, J. Cell. Biochem. 118 (2017) 629–639.
[46] M.Y. Lo, H.T. Kim, Chondrocyte apoptosis induced by hydrogen peroxide requires caspase activation but not mitochondrial pore transition, J. Orthop. Res. 22 (2004) 1120–1125.
[47] W. Zhang, E. Chen, M. Chen, C. Ye, Y. Qi, Q. Ding, H. Li, D. Xue, X. Gao, Z. Pan, IGFBP7 regulates the osteogenic differentiation of bone marrow-derived mesenchymal stem cells via Wnt/beta-catenin signaling pathway, Faseb. J. 32 (2018) 2280–2291.
[48] C. Ye, W. Hou, M. Chen, J. Lu, E. Chen, L. Tang, K. Hang, Q. Ding, Y. Li, W. Zhang, R. He, IGFBP7 acts as a negative regulator of RANKL-induced osteoclastogenesis and oestrogen deficiency-induced bone loss, Cell Prolif 53 (2020), e12752.
[49] W. Zhang, W. Hou, M. Chen, E. Chen, D. Xue, C. Ye, W. Li, Z. Pan, Upregulation of parkin accelerates osteoblastic differentiation of bone marrow-derived mesenchymal stem cells and bone regeneration by enhancing autophagy and beta-catenin signaling, Front Cell Dev Biol 8 (2020) 576104.
[50] K. Hu, B.R. Olsen, Osteoblast-derived VEGF regulates osteoblast differentiation and bone formation during bone repair, J. Clin. Invest. 126 (2016) 509–526.
[51] S. Kato, S.Y. Han, W. Liu, K. Otsuka, H. Shibata, R. Kanamaru, C. Ishioka, Understanding the function-structure and function-mutation relationships of p53 tumor suppressor protein by high-resolution missense mutation analysis, Proc. Natl. Acad. Sci. U. S. A. 100 (2003) 8424–8429.
[52] C. Ma, L. Wu, L. Song, Y. He, Safwat Adel Abdo Moqbel, S. Yan, K. Sheng, H. Wu, J. Ran, L. Wu, The pro-inflammatory effect of NR4A3 in osteoarthritis, J. Cell Mol. Med. 24 (2019) 930–940.
[53] Z. Cui, J. Crane, H. Xie, X. Jin, G. Zhen, C. Li, L. Xie, L. Wang, Q. Bian, T. Qiu, M. Wan, M. Xie, S. Ding, B. Yu, X. Cao, Halofuginone attenuates osteoarthritis by inhibition of TGF-β activity and H-type vessel formation in subchondral bone, Ann. Rheum. Dis. 75 (2016) 1714–1721.
[54] G. Zhong, X. Yang, X. Jiang, A. Kumar, H. Long, J. Xie, L. Zheng, J. Zhao, Dopamine-melanin nanoparticles scavenge reactive oxygen and nitrogen species and activate autophagy for osteoarthritis therapy, Nanoscale 11 (2019) 11605–11616.
[55] W. Zhang, D. Xue, H. Yin, S. Wang, C. Li, E. Chen, D. Hu, Y. Tao, J. Yu, Q. Zheng, X. Gao, Z. Pan, Overexpression of HSPA1A enhances the osteogenic differentiation of bone marrow mesenchymal stem cells via activation of the Wnt/beta-catenin signaling pathway, Sci. Rep. 6 (2016) 27622.
[56] J.A. vdS, R.G. G, A.J. vdL, S.K. B, R. K, J. D, The reliability of the Mankin score for osteoarthritis, J. Orthop. Res. : official publication of the Orthopaedic Research Society 10 (1992) 58–61.
[57] N. Gerwin, A.M. Bendele, S. Glasson, C.S. Carlson, The OARSI histopathology initiative - recommendations for histological assessments of osteoarthritis in the rat, Osteoarthritis Cartilage 18 (Suppl 3) (2010) S24–S34.
[58] H. Yao, J.K. Xu, N.Y. Zheng, J.L. Wang, S.W. Mok, Y.W. Lee, L. Shi, J.Y. Wang, J. Yue, S.H. Yung, P.J. Hu, Y.C. Ruan, Y.F. Zhang, K.W. Ho, L. Qin, Intra-articular injection of magnesium chloride attenuates osteoarthritis progression in rats, Osteoarthritis Cartilage 27 (2019) 1811–1821.
[59] V. Krenn, L. Morawietz, G.R. Burmester, R.W. Kinne, U. Mueller-Ladner, B. Muller, T. Haupl, Synovitis score: discrimination between chronic low-grade and high-grade synovitis, Histopathology 49 (2006) 358–364.
[60] L. Cinque, A. Forrester, R. Bartolomeo, M. Svelto, R. Venditti, S. Montefusco, E. Polishchuk, E. Nusco, A. Rossi, D.L. Medina, R. Polishchuk, M.A. De Matteis,

C. Settembre, FGF signalling regulates bone growth through autophagy, Nature 528 (2015) 272–275.
[61] M. Kapoor, J. Martel-Pelletier, D. Lajeunesse, J.P. Pelletier, H. Fahmi, Role of proinflammatory cytokines in the pathophysiology of osteoarthritis, Nat. Rev. Rheumatol. 7 (2011) 33–42.
[62] C. L, Z. Z, P. H, W. J, B. EA, S. L, Z. M, H. P, E.C. C, J. J, C.T. C, X. Z, K. T, C. S, Neural EGFL like 1 as a potential pro-chondrogenic, anti-inflammatory dual-functional disease-modifying osteoarthritis drug, Biomaterials 226 (2020) 119541.
[63] X. Chen, C. Zhang, X. Wang, S. Huo, Juglanin inhibits IL-1β-induced inflammation in human chondrocytes, Artificial cells, nanomedicine, and biotechnology 47 (2019) 3614–3620.
[64] C. C, M. L, T. W, H. S, A.S. C, G. C, O.D. K, B.N. C, Endogenous adenosine maintains cartilage homeostasis and exogenous adenosine inhibits osteoarthritis progression, Nat. Commun. 8 (2017) 15019.
[65] Y.E. Henrotin, S.X. Zheng, A.H. Labasse, G.P. Deby, J.M. Crielaard, J.Y. Reginster, Modulation of human chondrocyte metabolism by recombinant human interferon, Osteoarthritis Cartilage 8 (2000) 474–482.
[66] J. Ran, C. Ma, K. Xu, L. Xu, Y. He, S.A.A. Moqbel, P. Hu, L. Jiang, W. Chen, J. Bao, Y. Xiong, L. Wu, Schisandrin B ameliorated chondrocytes inflammation and osteoarthritis via suppression of NF-kappaB and MAPK signal pathways, Drug Des. Dev. Ther. 12 (2018) 1195–1204.
[67] Z. Luo, B. Zheng, B. Jiang, X. Xue, E. Xue, Y. Zhou, Peiminine inhibits the IL-1β induced inflammatory response in mouse articular chondrocytes and ameliorates murine osteoarthritis, Food & function 10 (2019) 2198–2208.
[68] F.F. Sun, P.F. Hu, Y. Xiong, J.P. Bao, J. Qian, L.D. Wu, Tricetin protects rat chondrocytes against IL-1beta-induced inflammation and apoptosis, Oxid Med Cell Longev (2019), 4695381, 2019.
[69] C.H. Ma, C.H. Wu, I.M. Jou, Y.K. Tu, C.H. Hung, P.L. Hsieh, K.L. Tsai, PKR activation causes inflammation and MMP-13 secretion in human degenerated articular chondrocytes, Redox Biol 14 (2018) 72–81.
[70] R. Liu-Bryan, Inflammation and intracellular metabolism: new targets in, OA. Osteoarthritis Cartilage 23 (2015) 1835–1842.
[71] A. Oeckinghaus, S. Ghosh, The NF-kappaB family of transcription factors and its regulation, Cold Spring Harb Perspect Biol 1 (2009) a000034.
[72] D. I, K.N. M, A. T, Epigenetic regulation of leptin affects MMP-13 expression in osteoarthritic chondrocytes: possible molecular target for osteoarthritis therapeutic intervention, Ann. Rheum. Dis. 66 (2007) 1616–1621.
[73] Y. Y, T.E. M, A. G, N.E. L, D. C, M. J, J. B, C.J. S, A. D, I. S, J. T, M.C. H, Lorecivivint, a novel intra-articular CLK/DYRK1A inhibitor and Wnt pathway modulator for treatment of knee osteoarthritis: a phase 2 randomized trial, Arthritis & rheumatology 72 (2020) 1694–1706.
[74] A.C. L, B.L. S, J.M. B, M.A. K, H. W, L. H, C. H, S.A. A, A.S. A, B.A. A, Modulating hedgehog signaling can attenuate the severity of osteoarthritis, Nat. Med. 15 (2009) 1421–1425.
[75] S.H. Chang, D. Mori, H. Kobayashi, Y. Mori, H. Nakamoto, K. Okada, Y. Taniguchi, S. Sugita, F. Yano, U.I. Chung, J.R. Kim-Kaneyama, M. Yanagita, A. Economides, E. Canalis, D. Chen, S. Tanaka, T. Saito, Excessive mechanical loading promotes osteoarthritis through the gremlin-1-NF-kappaB pathway, Nat. Commun. 10 (2019) 1442.
[76] A. Acevedo, C. Gonzalez-Billault, Crosstalk between Rac1-mediated actin regulation and ROS production, Free Radic. Biol. Med. 116 (2018) 101–113.
[77] T. KT, Transcription factor KLF2 and its role in the regulation of inflammatory processes, Biochemistry Biokhimiia 85 (2020) 54–67.
[78] H.J. M, H. D, L. L, A. Z, Biochemical and metabolic abnormalities in articular cartilage from osteo-arthritic human hips. II. Correlation of morphology with biochemical and metabolic data, The Journal of bone and joint surgery American 53 (1971) 523–537.